Third AO4ELT Conference - Adaptive Optics for Extremely Large Telescopes
Florence, Italy. May 2013
ISBN: 978-88-908876-0-4
DOI: 10.12839/AO4ELT3.13388

INTEGRATION AND LABORATORY CHARACTERIZATION OF THE ARGOS LASER GUIDE STAR WAVEFRONT SENSORS

Lorenzo Busoni[1a], Marco Bonaglia[1], Luca Carbonaro[1], Tommaso Mazzoni[1], Jacopo Antichi[1], Simone Esposito[1], Gilles Orban de Xivry[2], and Sebastian Rabien[2]

[1] INAF - Osservatorio di Arcetri, L.go E. Fermi 5, 50125 Firenze, Italy
[2] Max-Planck-Institut für extraterrestrische Physik, Giessenbachstrasse 1, 85748 Garching, Germany

Abstract. The integration status of the ARGOS wavefront sensors is presented. ARGOS is the laser guide star AO program for the LBT. It will implement a Ground Layer AO correction for the instruments LUCI, an infrared imager and multi-object spectrograph, using 3 pulsed low-altitudes Rayleigh beacons for each LBT's eye. It profits of the LBT's adaptive secondary mirrors and of FLAO's pyramid unit for NGS sensing. Each LGS is independently stabilized for on-sky jitter and range-gated using custom Pockels cells and then sensed by a 15 × 15 Shach-Hartman wavefront sensor. The 3 pupil images are reimaged on a single lenslet array and a single detector. In the WFS are also installed 3 patrol cameras for the acquisition of the laser beacons, a system for the stabilization of the pupil images on the lenslet array and an internal source for calibration purposes. The two units are now completing the integration phase in Arcetri premises. We describe the characterization of the units and the closed-loop test realized using a deformable MEMS mirror.

1 Introduction

The LBT laser guide star program (ARGOS) foresees the implementation of 3 pulsed Rayleigh beacons for each eye of the telescope [5]. The 532*nm* laser light will be focused at 12*km* altitude through a refractive launch system, arranged on a triangular asterism inscribed in a 2′ radius circle. This will allow to effectively sense the ground layer turbulence above the LBT site using a dedicated LGS wavefront sensor (LGSW).

The LGSW is a 15 × 15 subapertures Shack-Hartmann wavefront sensor, provided with Pockels cell type optical shutters to shrink the LGS spot elongation and of pupil-conjugated fast steering mirrors to compensate for the independent LGS jitter. An optimized optical design for the LGSW allows to arrange the 3 LGS on a single large detector having 264 × 264 pixels developed by PnSensors in collaboration with MPE [6]. A set of motorized lenses keep fixed on the lenslet array the pupil position on each LGS light path compensating mechanical flexure.

The LGSW will allow to measure the ground layer turbulence up to 150 modes providing a GLAO correction through the LBT adaptive secondary mirror. In the ARGOS system the tip-tilt indetermination is solved picking up a natural guide star with a dedicated quad-cell wavefront sensor installed inside the FLAO pyramid WFS [3]. In this way ARGOS will act as a seeing enhancer for the LBT, providing a reduction of the median seeing by a factor 2-3 and hence bringing to a gain of a factor 4-9 in observing time for the two LUCI near-infrared imagers and spectrographs.

[a] lbusoni@arcetri.astro.it

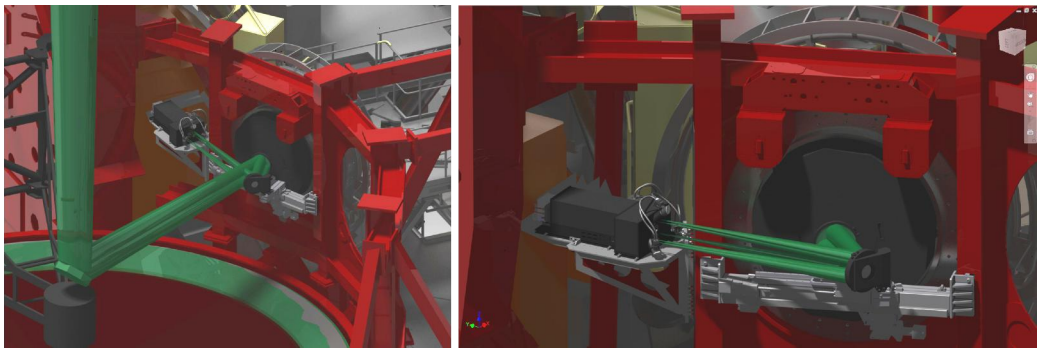

Fig. 1. Left: model of the LBT rotator gallery where the instruments are mounted. At the LUCI focal station ARGOS will install a laser pick-off system and a dedicated LGS wavefront sensor. Right: close up view of the ARGOS hardware: the laser pick-off system is composed by a dichroic beamsplitter and a fold mirror mounted on slidable supports. The LGSW is installed on an auxiliary platform aside the LUCI focal station.

Figure 1 shows a model of the telescope rotator gallery, where the science instruments are mounted and are fed by the telescope light rotating the tertiary mirror. ARGOS will add a mechanical interface just in front of the LUCI rotator to support a laser pick-off system, detailed in section 2. This system reflects the laser light toward the LGSW, installed on a dedicated interface next to the LUCI focal station. Section 3 describes the test currently ongoing at Arcetri premises on the 2 fully assembled LGSW units.

2 Laser pick-off system

Figure 1 shows that the new solution for the pick-off system requires a particular positioning of a folding mirror with respect to the LBT primary mirror. The impact of this solution has been fully analysed and considered as a reasonable compromise in terms of mechanical complexity and system performance. Hence, the laser pick-off system of ARGOS is now composed by two elements: a 320mm diameter double-flat dichroic, wedged by 0.08° and tilted by 15° with respect to the LUCI optical axis and a 12″ diameter flat mirror folded by 21° which redirects the laser light reflected by the beam splitter toward the LGSW.

Both the dichroic and the folding mirror have custom dielectric coatings which allow to obtain the best reflection efficiency of the s-polarized light at 532nm and, in case of the dichroic, the requested performances of transmission toward LUCI of the visible/infrared wavelengths above 620nm.

2.1 Dichroic and fold mirror production and testing

Three dichroic units have been commissioned to Laser Zentrum Hannover (LZH). This company has been selected after a decision process based on 2 caveat : the capability to deal both with the polishing and coating of optics bigger than 300mm diameter with 20mm thickness and a small delivery time, as requested by the ARGOS consortium plan.

Figure 2 shows one of the dichroic units produced by LZH. The surface error measurement on the 3 units (specified as DIC 01, 02, 03) is reported in Table 1 and it shows that at least 2 optics match the tighter specifications imposed to these units by our wavefront budget analysis.

These measurements will be repeated after the coating is deposed on both sides of the dichroics and again after the 3 complete units have undergone a full thermal and humidity cycle in order to verify the very low stress requested by design.

Fig. 2. Left: picture of one of the ARGOS dichroics before the coating process. Right: measure of the third dichroic surface error performed at LZH on a 90*mm* diameter patch. The surface PtV amounts to 1/8 waves, mainly due to an astigmatism term.

Table 1. Surface error (SE) measurements of the 3 ARGOS dichroics before the coating process. The goal specification for the SE rms is 50*nmrms*.

Sub. ♯	**Meas. SE PtV** [*nm*]	**Meas. SE rms** [*nm rms*]	**Meas. SE PtV/rms**
DIC 01	204.1	52.7	3.87
DIC 02	113.0	23.6	4.79
DIC 03	78.0	19.3	4.05

Due to the tight coating specifications, LZH selected the ion assisted deposition technique as the best option for coating deposition together with the precaution of a both-sided multi-layers deposition strategy, that minimizes stress over the dichroic surface, then minimizing its surface error at low/medium spatial frequencies. This process, together with the pre-coating polishing, is mandatory to obtain small errors in the full dichroic MTF bandwidth. Figure 3 highlights the transmission properties of the coating designed for the ARGOS dichroics and measured on a witness sample.

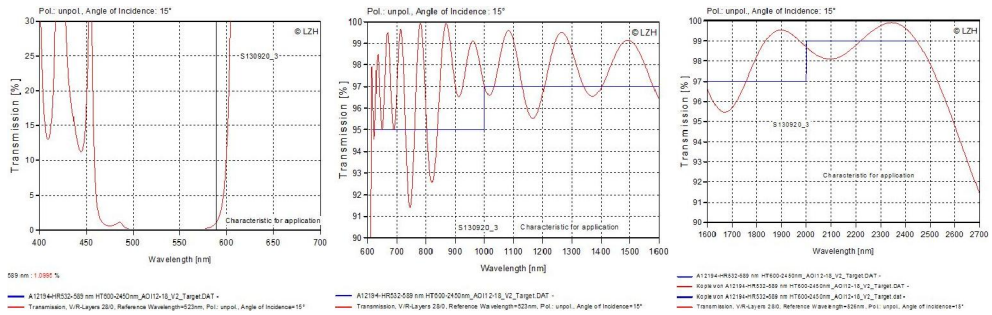

Fig. 3. Transmission curves of the dichroic coating deposited and measured on a witness sample.

2.2 Laser pick-off mechanical support

The mechanical support for the ARGOS laser pick-off system is shown in Figure 4. It consists of different structures, mechanisms, motors and electronics, to support and displace both the dichroic and the fold mirror between their parking positions and the operational position. The 2 optics are fixed to supporting cells that are finely adjustable in position and orientation. The dichroic cell sits on a carriage that translates over 2 rails along the main support structure. The fold mirror cell is attached to a rotational arm. The main support structure is directly bolted in front of the LUCI focal station, where dedicated interface plates have already been placed.

Fig. 4. Picture of the ARGOS laser pick-off support structure assembled at Tomelleri s.r.l. premises. The 2 cells are holding aluminium dummies of the optics to test the stability of the structure under different gravity conditions. Picture on left shows the parked position for the optics while on the right it shows their working positions.

The support structures for both eyes of the telescope have been commissioned to Tomelleri s.r.l. and are actually undergoing functionality and stability tests. Thermal cycling and stress test have also been scheduled to ensure the durability of the structure under the different telescope environments.

3 The laser guide star wavefront sensor

The atmospheric turbulence in the direction of the 3 LGS is sensed through a dedicated wavefront sensor. As shown in Figure 1 this device takes place aside the LUCI focal station where the telescope images a $12km$ distant source. The ARGOS LGSW is composed by different devices, a complete description can be found in [2].

Two units of the ARGOS LGSW have been assembled at Arcetri premises. Figure 5 shows the 2 units on their test benches. Actually one of the units is used to perform AO closed loop tests. At this scope a 140 actuator MEMS Multi DM produced by Boston Micromachines has been installed on the pupil-conjugate plane of the internal light source (see section 3.1). The second LGSW instead is used to test the stability of the opto-mechanical layout and the performance of the LGSW internal control loops (see section 3.2).

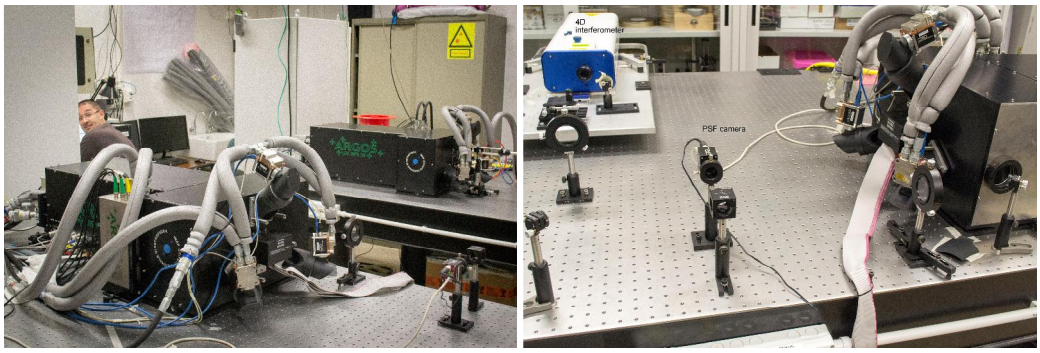

Fig. 5. Left: picture of the 2 ARGOS LGSW addembled at Arcetri premises. The front one is the DX unit used to simulate an AO closed loop with a MEMS DM. The back one is the SX unit used to perform the stability test and to check the functionality of the LGSW control loops. Right: to have a direct feedback of the MEMS DM surface during the AO loop tests the light coming from a 4D interferometer is directed inside the LGSW by the use of few transfer optics. The laser beam is also focused on a Prosilica GC1350 camera to simulate an on-axis source.

3.1 AO closed loop test

Figure 5 shows on right the optical setup used for the AO closed loop tests. A MEMS DM has been installed on the internal light source of the DX LGSW unit and it is controlled via USB by a laptop PC connected to the laboratory network.

To have a feedback of the MEMS surface figure during the test it has been necessary to add an on-axis source to the LGS asterism. The light producing the on-axis source is provided by a 4D Phasecam 4020 interferometer. The $6mm$ diameter collimated laser beam is focussed and recollimated by two $500mm$ lenses, that allow to reimage the MEMS DM surface at the entrance of the 4D interferometer. Two flat mirrors allow to fit the optical setup on the optical bench surface and give a handy adjustment of the beam height and pupil position.

Inside the DX LGSW, just in front of the MEMS DM surface, it has been installed a cube beam splitter to direct the interferometer light toward the MEMS DM. The reflected light is then divided by a second beam splitter placed in between the 2 lenses where the light is focussed. Part of the light returns toward the interferometer and gives a slow rate direct feedback of the DM surface figure while the other part is imaged on a Prosilica GC1350 camera. In this way it is possible to have a faster feedback of the DM surface through the PSF image.

First the LGSW has been calibrated recording the Interation Matrix using a push-pull algorithm applying a set of 66 Karhune-Loeve modes to the MEMS-DM. The modal amplitude has been scaled to enhance the sensor signal-to-noise while not saturating the DM actuators' stroke. The slopes recorded by the 3 SH sensors have been concatenated and inverted using a pseudo-inversion algorithm to calibrate the system as a GLAO sensor.

The sensor measurement error has been evaluated in different flux regimes. In this test the system ran in open loop: the DM was set in its best flat position, evaluated minimizing the aberration on the PSF camera. In these condition the slope offset for the sensor were recorded and subtracted to the following 1000 slope measurements acquired at $1kHz$ rate. Figure 6 shows the standard deviation of the LGSW measurements decomposed on the modal basis. In high flux condition (over $5000ADU\ \ subap^{-1}\ \ ms^{-1}$) the integrated surface measurement error was $30nm\ rms$.

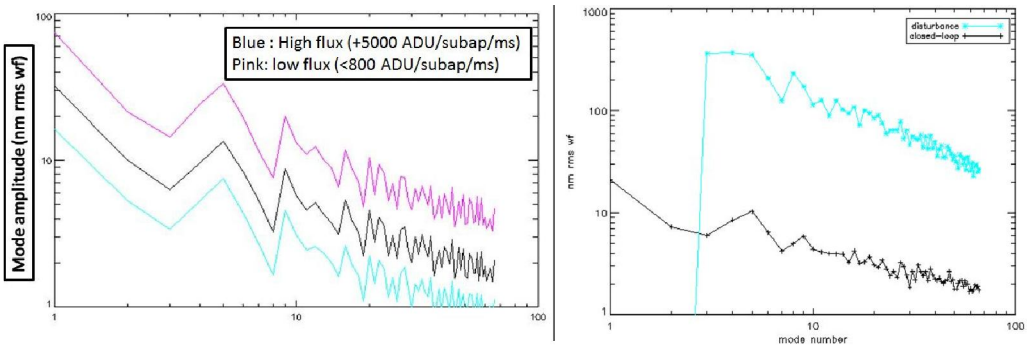

Fig. 6. Left: plot of the noise propagation in different flux conditions. The standard deviation of the modal amplitudes had been evaluated recording the LGSW slopes in open loop when a static shape was applied to the DM. Right: comparison of the open loop and closed loop residuals when the disturbance was applied to the mirror, equivalent to $r_0 = 10cm$ and windspeed = $10m\ s^{-1}$. The residual WF error is $50nm\ rms$.

The LGSW performance were also evaluated simulating an AO closed loop. In this test the MEMS-DM has been used to inject the wavefront disturb onto the LGSW mimiking a frozen turbulence equivalent to $r_0 = 10cm$ evolving with a wind speed of $10m\ s^{-1}$. At the same time the DM implemented the AO correction, so considering that the turbulence could only be injected in a pupil conjugate plane, the DM worked in a condition very close to the best flat shape. In these conditions the LGSW slopes recorded were used to estimate the residual wavefront error. The blue line plotted on right of Figure 6 shows the standard deviation of the wavefront disturb evolution over $3s$ integration decomposed on the modal basis. The tip-tilt terms were removed from the disturb to avoid saturating the mirror dynamical range. The black line shows the closed loop residuals evaluated from the LGSW slopes in high flux conditions, corresponding to a residual wavefront error of about $50nmrms$.

3.2 Pupil stabilization test

To compensate any mechanical flexure that can affect the position of the pupil in the LGSW, the system has been provided with a control loop that estimates the position of the pupils from the CCD frame. This has to be done independently for each one of the 3 LGS beams. The system has also the capability to independently re-adjust the position of each beam displacing a collimator held on a Newport M-461-XZ-M stage and actuated by 2 Newport NSA12 stepper motors.

To estimate the position of each pupil the flux over each subaperture is evaluated simply binning by 8 the CCD frame. In this way a 15×15 elements image of the pupil is obtained (see the first image in Figure 7). The pupil center is then measured performing the Hough Transform[1] of the binned image. At this scope 5 or 10 binned frames acquired at $1kHz$ are averaged, the integral flux over each subaperture amounting to 3000 ADU. The Hough Transform then detects a circle of a determined radius processing an histogram in the parameter space, instead of the image space.

The procedure to measure the pupil position can be explained in 3 steps. The first one is the edge-detection: the Sobel operator[4] is used. It returns the edge ($\mathcal{S}$) and the edge orientation (θ) values for each image. Then a circle is defined by the equation $(x-a)^2 + (y-b)^2 = r^2$.

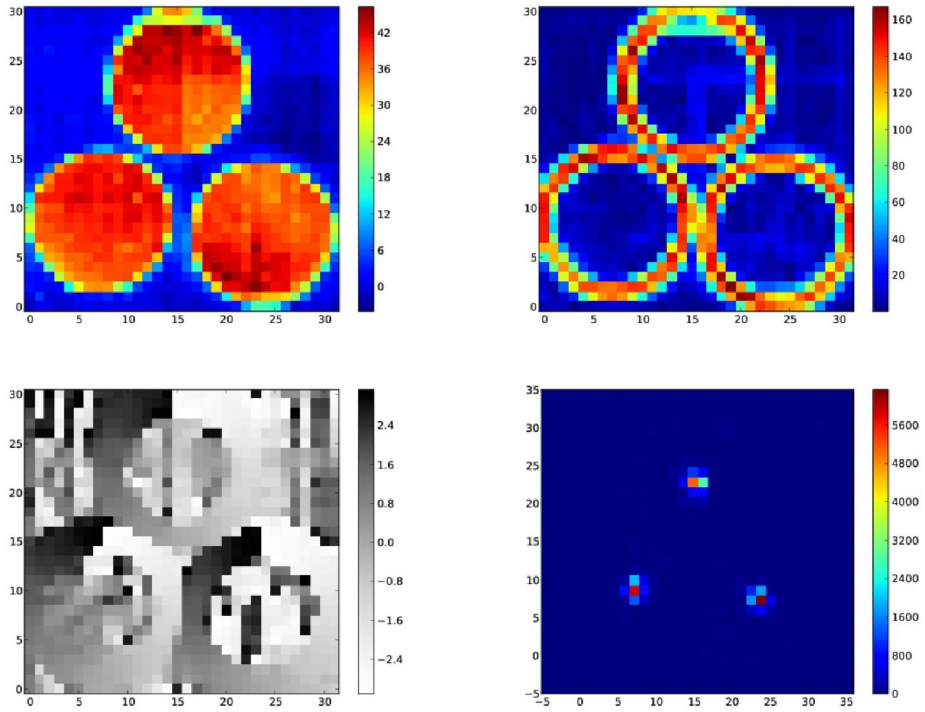

Fig. 7. Example of the image processing for the pupil center evaluation. Top left: starting image, top right: image convolved with Sobel operator ($\mathcal{S}$). Bottom left: Image convolved with Sobel operator, edge orientation (θ), bottom right: Hough transform of the image ($\mathcal{H}$).

The mapping from the image space (x, y) to parameter space (a, b, r)[1] is made by building an histogram ($\mathcal{H}$). A subaperture at the edge of the image $\mathcal{S}(\hat{x}, \hat{y})$ contributes in the parameter space in the point $(\hat{a}, \hat{b})$, where:

$$\begin{cases} a(x, y, r, \theta) = x - r\cos(\theta(x, y)) \\ b(x, y, r, \theta) = y - r\sin(\theta(x, y)) \end{cases}$$

$\mathcal{H}(a(x, y, r, \theta), b(x, y, r, \theta))$ is the sum of each pixel (x, y), mapped to (a, b), weighted by the values of the edge image $\mathcal{S}(x, y)$.

The construction of the histogram is the second step. The third one is the analysis of the histogram through the fit with a gaussian peak. To obtain a more robust procedure the analysis is repeated several times and the result of each analysis is evaluated upon the width and the height of the gaussian peak. In this way it has been possible to check the data quality setting a threshold on the fit parameters and discarding corrupted data, for example when the LGS is lost, giving to a more robust and stable algorithm. In addition the possibility to average fit parameters from different measurements improves the algorithm accuracy, because of the imprecision of the single fit procedure.

This algorithm has been tested in the laboratory using the SX LGSW unit. First the interaction matrix between the lens motors and the measurement algorithm has been recorded. The difference between the measured center and the target center has been defined as centering error. When the stabilization loop is closed the product of the centering error by the inverse of the interaction matrix gives the command for the pupils motors.

[1] in this case $r = 7.5$ subapertures.

Figure 8 shows the variation of the centering error over 1 hour of closed loop operation. Measurements along the X and Y axis of each LGS pupil have been acquired at 10s interval in conditions of high light flux ($> 5000 ADU\ \ subap^{-1}\ \ ms^{-1}$). The green line highlights the accuracy requirement for the pupil stabilization loop of 0.1$subap$, the measurement errors were below this threshold for the entire closed loop operation. Further work is needed to study the algorithm behaviour under different light conditions.

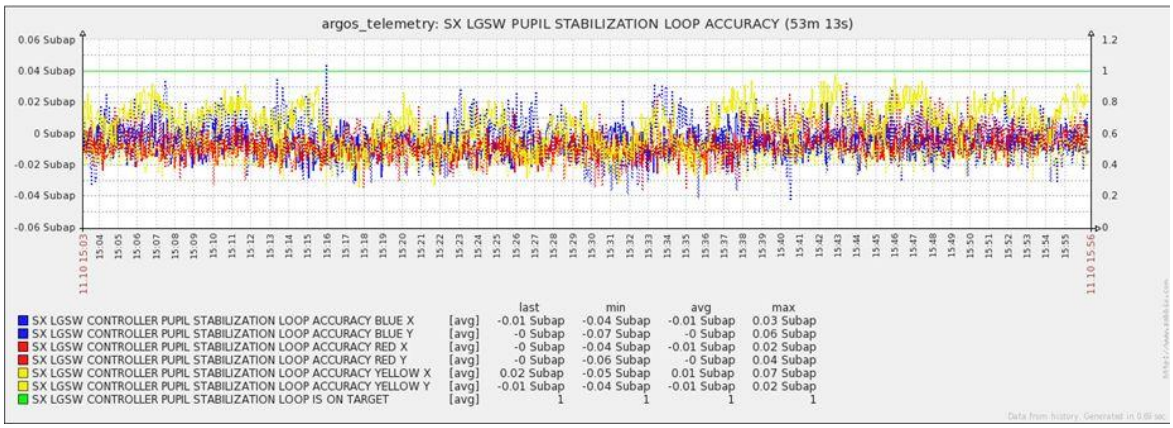

Fig. 8. Plot of the centering error standard deviation when the pupil stabilization loop was closed on the SX LGSW. Values for 1 hour of operation are shown at 10s interval. The green line shows the accuracy requirement of 0.1$subap$.

4 Conclusions

We have presented in this paper an up to date status of the ARGOS wavefront sensing units and of the laser pickoff system. Most of the parts have already been produced and are currently ongoing their acceptance tests: the dichroic optic has been polished meeting the tight surface error speicifications, its mechanical support has been completely assembled and its functionalities checked. The 2 LGSW units are fully assembled at Arcetri premises, one of them is used to simulate an AO correction loop using a MEMS-DM. Preliminary results shown that in lab conditions and high flux regimes it is able to give a 30$nm\ rms$ accuracy in the WF measurement at 1kHz rate.
In parallel on the other LGSW unit the internal loops are developed and tested: an example is the pupil recentering loop that uses an algorithm based on the Hough transform. The test shown that it is able to keep fixed the pupil position with an accuracy better than 0.03 subap, below the requirement level of 0.1 subap.

References

1. Ballard, D. H., Generalizing the hough transform to detect arbitrary shapes, **Readings in computer vision: issues, problems, principles, and paradigms**, Fischler, Martin A. and Firschein, Oscar (1987).
2. Bonaglia, M. et al., Laboratory characterization of the ARGOS laser wavefront sensor, **2012SPIE.8447E..6BB** (2012).

3. Esposito, S. et al., Natural guide star adaptive optics systems at LBT: FLAO commissioning and science operations status, **2012SPIE.8447E..0UE** (2012).
4. Hadwiger, M. et al., **Real-time Volume Graphics** (2006).
5. Rabien, S. et al., ARGOS: the laser guide star system for the LBT, **2010SPIE.7736E..12R** (2010).
6. Orban de Xivry, G. et al., A test bench for ARGOS: integration of sub-systems and validation of the wavefront sensing, **2012SPIE.8447E..51O** (2012).